RSC Advances

PAPER

Cite this: *RSC Adv.*, 2021, **11**, 31712

Preparation and characterization of an imogolite/chitosan hybrid with pyridoxal-5′-phosphate as an interfacial modifier†

Masaru Mukai, [a] Akihiko Takada, [a] Ayumi Hamada,[a] Tomoko Kajiwara[ab] and Atsushi Takahara *[ab]

Received 20th June 2021
Accepted 13th September 2021

DOI: 10.1039/d1ra04774d

rsc.li/rsc-advances

Imogolite/chitosan hybrid films were prepared using pyridoxal-5′-phosphate (PLP) as an interfacial modifier. Thermogravimetric analysis and spectroscopic measurements revealed that the phosphate group of PLP was adsorbed on the imogolite. Furthermore, rheological measurements suggested that the PLP-modified imogolites (PLP–imogolite) had strong interactions with chitosan in solution. Moreover, UV absorption of the hybrid film showed that PLP and chitosan formed Schiff base linkages. Therefore, the hybrid films exhibited a significant improvement in their mechanical properties compared to those of pristine chitosan/imogolite hybrid films.

Introduction

Imogolite is an aluminum silicate mineral consisting of nanotube structures that have a diameter of 1.8–2.2 nm and a length of several micrometers.[1–3] It was discovered by Yoshinaga and Aomine (1962) in the volcanic ash soil of South Kyushu, Japan.[4] Nowadays, imogolite is found in areas where the volcanic ash is weathered by rainfall.[5,6] However, it has also been synthesized under relatively mild conditions.[7] Imogolite has been considered a promising nanomaterial and gained attention as a naturally occurring functional nanomaterial owing to its unique structure with a high aspect ratio.[8] It is expected to be used for various applications such as adsorbent materials,[9] enzyme immobilization,[10] fuel storage media[11] and so on.[12,13] Over the past few years, we have been studying imogolite based organic–inorganic hybrid materials.[10,14–19] Owing to its large surface ratio and high aspect ratio, imogolite has been used to reinforce polymer matrices for polymer hybrids.[13,14]

Chitosan is a linear polysaccharide that can be obtained from the exoskeleton of crustaceans. Therefore, it is regarded as an eco-friendly, biocompatible, and biodegradable material.[20–25] Although chitosan and imogolite are unique materials, their hybrids are not reported. Furthermore, chitosan and imogolite are positively charged under near-neutral pH and exhibit repulsive interactions when interfacial modifiers are absent.[14,26]

In this study, pyridoxal-5′-phosphate (PLP) was used as an interfacial modifier for imogolite/chitosan hybrid for the following reasons: (1) PLP is a metabolically active form of vitamin B6 and has a low environmental impact. (2) The aldehyde groups of PLP are expected to form Schiff base linkage with the amino groups of chitosan in a weak acid solution.[27–31] (3) Phosphate groups interact strongly with the outer surface of the imogolite (Al-OH).[10,15–18] Moreover, the interfacial interaction can be directly visualized from the spectral changes associated with the PLP–Schiff base formation.[27–30]

Brunauer–Emmett–Teller (BET) specific surface area of imogolite (200–400 $m^2\ g^{-1}$)[14,26] is larger than that of nano-compounds, such as halloysite (80–150 $m^2\ g^{-1}$),[14,26] allophane (140–180 $m^2\ g^{-1}$),[32] montmorillonite (30–130 $m^2\ g^{-1}$),[32] and carbon nanotubes (15–250 $m^2\ g^{-1}$).[26] Since inner diameter of imogolite is 1 nm and tube interior chemistry of imogolite is silica tetrahedrons,[14] PLP modification of the inner surface of imogolite could not be achieved. Assuming an outer diameter of 2 nm and inner diameter of 1 nm, the area of the outer surface of imogolite is estimated to be 130–270 $m^2\ g^{-1}$, which is still relatively large compared to other nano-compounds. Because the interaction between the filler and the polymer matrix affects the mechanical strength of the composite material, it is assumed that imogolite would benefit greatly from the interfacial modifier. Fig. 1 shows a schematic representation of the preparation of imogolite/chitosan hybrid films.

Materials and methods

Materials

Chitosan and PLP were purchased from Tokyo Chemical Industry Co., Ltd. Acetic acid, sodium hydroxide, hydrochloric acid, zinc chloride, and cadmium chloride 2.5-hydrate were purchased from FUJIFILM Wako Pure Chemical Corp. Since the physical and chemical properties of synthetic imogolite using

[a]*Institute for Materials Chemistry and Engineering, Kyushu University, 744 Motooka, Nishi-ku, Fukuoka 819-0395, Japan. E-mail: takahara.atsushi.150@m.kyushu-u.ac.jp*
[b]*Research Center for Negative Emission Technology, Kyushu University, 744 Motooka, Nishi-ku, Fukuoka 819-0395, Japan*

† Electronic supplementary information (ESI) available. See DOI: 10.1039/d1ra04774d

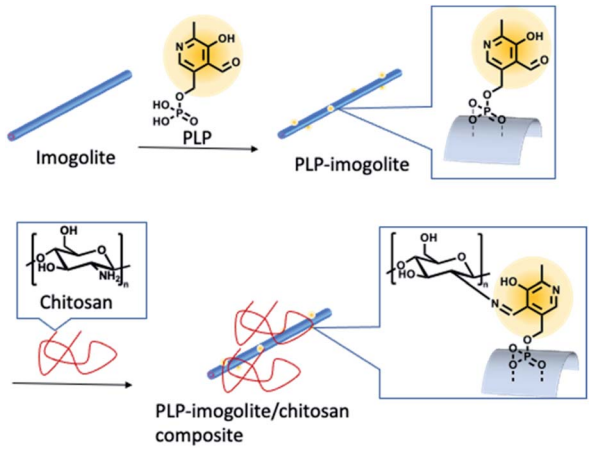

Fig. 1 Schematic representation of PLP modification of imogolite surface and preparation of imogolite/chitosan hybrid films.

Farmer *et al.* reported method have been well investigated, we synthesized imogolite by his method.[7]

Surface modification of imogolite with PLP

Imogolite (60 mg) was dispersed in 200 mL water *via* sonication for 1 h. Subsequently, PLP (60 mg) was added to the solution and stirred for 12 h at room temperature in the dark to minimize the photodecomposition of PLP.[33] The excess PLP was removed by placing the solution in a 6–8 kD dialysis bag (Spectra/Por 1, Standard RC Tubing, Repligen Corp., MA, U.S.A.). The solution was dialyzed at room temperature for 4 d. The dialysate was replaced with fresh water daily. On the final day, spectroscopic measurements confirmed no PLP-derived adsorption in the dialysate. Further, yellow cotton-like PLP-modified imogolite (PLP–imogolite) was obtained *via* freeze-drying. Fig. S1 and S2† (1.5 μm × 1.5 μm) show images of the PLP–imogolite and scanning force microscopy (SFM) images of the unmodified imogolite and PLP–imogolite, respectively.

Preparation of imogolite/chitosan hybrid film

Chitosan (1 g) was dissolved in 30 mL 2% aqueous acetic acid solution. Ethanol (20 mL) was added to the mixture and stirred well. Subsequently, 5 mL of the chitosan solution was transferred to a round-bottom flask (5 cm in diameter). Thereafter, a 10 mL aqueous solution of PLP–imogolite or pristine imogolite was added to the flask and mixed. The mixture was placed in a glass Petri dish. The samples were dried in a desiccator for 7 d in the dark and under vacuum at room temperature. Consequently, a translucent yellow film was obtained (Fig. S3†).

Characterization

UV absorption spectra were obtained using a UV spectrophotometer (UV-3600, Shimadzu Corp., Kyoto, Japan) in the 200–600 nm region. Thermogravimetric analysis (TGA) of the pristine imogolite and PLP–imogolite samples was conducted. Each sample was placed in an aluminum pan and heated from 273 K to 873 K at 10 K min^{-1} (TG/DTA6200, Seiko Instruments Inc., Chiba, Japan). The morphologies were visualized using SFM (SPA400, Seiko Instruments Inc., Chiba, Japan). Zeta potential measurements were performed using an electrophoretic light-scattering spectrophotometer (ELS-Z2, Otsuka Electronics Co., Ltd, Tokyo, Japan) with a standard cell at room temperature (pH 7). Tensile testing was conducted using an EZ-L (Shimadzu Corp., Kyoto, Japan) with a 1 kN load cell under a relative humidity of 10–15% at 298 K. These tests were conducted at a stretching speed of 1 mm min^{-1} on a sample with a gauge length of 20 mm. Fourier transform infrared (FT-IR) spectra were recorded on VERTEX 70 (Bruker Co. Ltd, Massachusetts, USA). IR samples were prepared by KBr pellet method. Rheological tests were performed using a Physica MCR 101 rheometer (Anton Parr, Graz, Austria) with a parallel-plate geometry (diameter 50 mm; gap length 1 mm) at 298 K. The concentration of the pristine chitosan solution was 4 wt% in a 2 wt% aqueous acetic acid solution. To prepare pristine imogolite/chitosan solution or PLP–imogolite/chitosan solution, identical volumes of 4 wt% chitosan solution and 1 wt% pristine imogolite or PLP–imogolite solution were mixed.

Results and discussion

Characterization of the PLP–imogolite interaction

The surface modification of the imogolite with PLP was confirmed through UV-vis spectrometry, zeta potential measurement, FT-IR spectrometry, and TGA. Fig. 2 shows the UV absorption spectra of pristine-imogolite, pure PLP and PLP–imogolite aqueous solution. No absorption peak was observed for the pristine imogolite (Fig. 2, red line). Meanwhile, PLP–imogolite (Fig. 2, blue line) showed absorption peaks at 330 nm and 388 nm, which were assigned to PLP (Fig. 2 black line).[34,35] The increase in absorbance at 330 nm compared to 388 nm indicated a decreased dispersibility in water and increased light scattering of PLP–imogolite. The change in dispersibility suggests an interaction between imogolite and PLP. The zeta potential measurements was carried out to reveal the interaction between PLP and imogolite. The zeta potential of pristine imogolite was 37 ± 3.1 mV, which reduced to 12.0 ± 2.5 mV

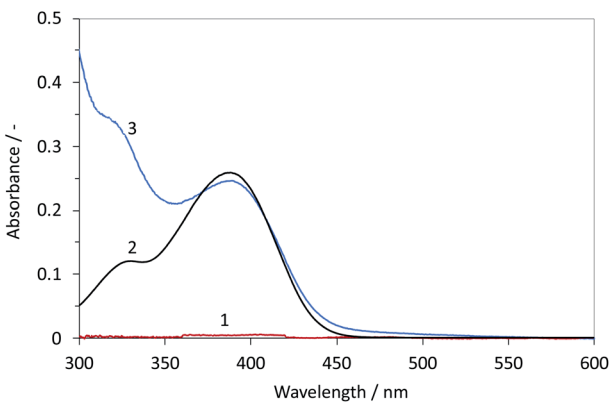

Fig. 2 Absorption spectra of 0.3 mg mL^{-1} pristine imogolite (1, red line), 50 μM PLP in potassium phosphate buffer (pH 7.5) (2, black line) and 0.3 mg mL^{-1} PLP–imogolite (3, blue line).

after modification. This indicates an interaction between PLP and the surface of the imogolite.

FT-IR spectra of pristine imogolite, pure PLP, PLP–imogolite, are shown Fig. S4.† The absorption peaks at 3499, 995 and 940 cm^{-1} are ascribed to stretching vibration of O–H, Si–O and Al–O in the pristine imogolite, respectively. The absorption peaks at 1646, 1554, 1244, 1152, 1039 and 978 cm^{-1} in FT-IR spectrum of pure PLP ascribed to C=O vibration, pyridine ring stretching vibration, P=O vibration, antisymmetric vibration of PO_2^-, antisymmetric vibration of $P(OH)_2$, symmetric vibration of PO_2^-, respectively.[36] In the FT-IR spectra of the PLP–imogolite, both PLP-derived peaks and imogolite-derived peaks were observed. This result suggested that the adsorption of PLP on the imogolite surface. The amount of PLP adsorbed was determined from the TGA curves before and after PLP adsorption (Fig. S5†). The results confirmed that 2.3 wt% of PLP was adsorbed on the imogolite. Assuming that the surface area of imogolite is 130–270 $m^2 g^{-1}$, the density of adsorbed PLP is calculated as 0.21–0.44 molecules per nm^2.[14] The decomposition temperature of PLP confirmed that the decomposition began at approximately 410 K (Fig. S6†). Because of the low decomposition temperature, it was difficult to evaluate the thermal characteristics of the hybrid films using differential scanning calorimetry and dynamic mechanical analysis at temperatures above 410 K. Therefore, Schiff base formation and precipitation were characterized *via* spectroscopic analysis and rheological measurements as these analytical methods which do not involve thermal decomposition.

Rheological measurements of mixed solutions

Rheological measurements were performed 24–48 h after the preparation of the mixed solutions. The solutions were sonicated for 30 min before the measurement. While all solutions were viscous, the PLP–imogolite/chitosan solution was more viscous and sticky. Fig. 3 shows the results of the steady-state shear viscosity measurements at different shear rates. The viscosity for pristine-imogolite/chitosan solution increased slightly with the addition of pristine imogolite. In contrast, viscosity of the PLP–imogolite/chitosan solution was approximately one order of magnitude higher than that of the pristine-imogolite/chitosan solution. Moreover, the shear rate dependence of viscosity of the PLP–imogolite/chitosan solution was fairly different from that of pristine-imogolite/chitosan. For all three solutions, the viscosity decreased with increasing the shear rate. Such a dependence is called shear thinning behavior. This behavior implies that shear flow induces a structural change of the system such as destruction of network structure or a change of flow state such as change of molecular orientation under flow. Only this flow experiments did not give us enough information to discuss association structure in solution in detail. However, these rheological differences in the presence of PLP indicate that the dispersion state of imogolite is different between the solutions, which arises from the Schiff base-bond formation between chitosan and imogolite.

Characterization of hybrid film

The spectral changes associated with the PLP–Schiff base formation have been extensively studied. The peak near 330 nm and the peak at 420 nm of PLP–Schiff base are derived from enolimine form and ketoenamine form, respectively.[37–39] The intensity ratio of the two peaks changes depending on the environment, however, there is very little shift change.[38–40] Therefore, on the basis of absorption peak positions, the formation of Schiff bases could be discussed without distinguishing between film (Fig. 4) and solution (Fig. 2). Because the large absorbance was observed below 350 nm in the film (Fig. 4, blue line), and the peak around 330 nm is also observed in solution before Schiff base formation (Fig. 2, blue line), it is difficult to argue for Schiff base formation from the near 330 nm peaks. The PLP–imogolite solution showed an absorption peak at 388 nm (Fig. 2, blue line). Furthermore, the 25 wt% PLP–imogolite/chitosan film exhibited a 420 nm shoulder peak (Fig. 4, blue line). However, the shoulder peak was absent in the absorption spectra of the pristine-chitosan film, 25 wt% pristine-imogolite/chitosan film (Fig. 4, green line), or 0.3 mg mL^{-1} PLP–imogolite aqueous solution (Fig. 2, blue line). The

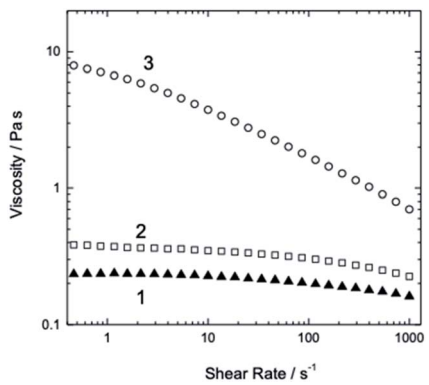

Fig. 3 Shear rate dependence of steady-state shear viscosity of the 2 wt% pristine-chitosan solution (1, ▲), pristine-imogolite/chitosan solution (2, □), and PLP–imogolite/chitosan solution (3, ○).

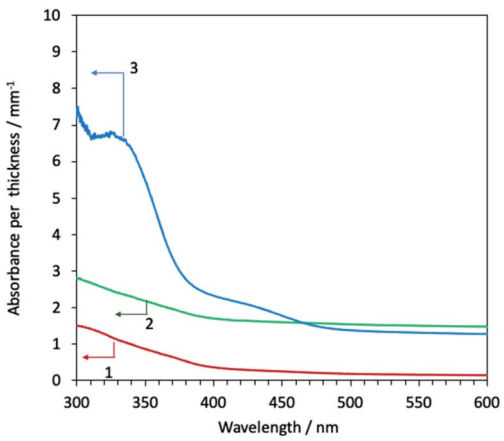

Fig. 4 Normalized UV absorption spectra of pristine-chitosan (1, red line), 25 wt% pristine-imogolite/chitosan (2, green line), and 25 wt% PLP–imogolite/chitosan (3, blue line) films.

Table 1 Mechanical properties of the hybrid films under tensile loading

	Young's modulus (GPa)	Tensile strength (MPa)	Elongation at break	Toughness (MJ m^{-3})
Pristine chitosan	0.34 ± 0.17	24 ± 8.5	0.16 ± 0.06	2.5 ± 2.5
25 wt% pristine-imogolite/chitosan	0.18 ± 0.13	19 ± 10	0.22 ± 0.01	2.6 ± 1.5
25 wt% PLP–imogolite/chitosan	0.70 ± 0.28	37 ± 4.1	0.15 ± 0.04	3.8 ± 1.0

peak shift from 388 nm peak in PLP–imogolite solution (Fig. 2, blue line) to 420 nm peak in the hybrid film (Fig. 4, blue line) suggests the formation of a Schiff base linkage between PLP and chitosan. The percentage of Schiff bases in the film was calculated from the molar absorption coefficient, considering the contribution of scattering. The absorption spectra of the free PLP and PLP–Schiff bases were ascribed to 4-(2-hydroxyethyl)-1-piperazineethanesulfonic acid (HEPES) and tris(hydroxymethyl) aminomethane (Tris) buffer solutions, respectively. HEPES buffer solution (100 mM pH 7.5) with 0.2 mM PLP had a typical free PLP absorption spectrum, while in Tris buffer solution (100 mM, pH 7.5) with 0.2 mM PLP, the Tris–PLP reaction forms the Schiff base linkage. The molar absorption coefficients of the free PLP (388 nm), PLP–Schiff bases (420 nm), and iso-absorption point (400 nm) were 4900 M^{-1} cm^{-1}, 5100 M^{-1} cm^{-1}, and 4800 M^{-1} cm^{-1}, respectively.[37] Calculations showed that 37% of the adsorbed PLP formed Schiff bases by binding to the amino groups of chitosan in the 25 wt% PLP–imogolite/chitosan film.

The mechanical properties of the hybrid films were characterized using a tensile test (Table 1, Fig. S7†). Toughness is defined as the area under the stress–strain curve. The mean values of Young's modulus, tensile strength, and toughness of the 25 wt% PLP–imogolite/chitosan film are 2, 1.5, and 1.5, respectively, larger than those of the pristine-chitosan film. In particular, Young's modulus showed sufficient improvement even after taking into account the error. Conversely, a decrease in the mean values of Young's modulus, tensile strength, and toughness was observed in the chitosan system with 25 wt% pristine imogolite. These results suggest that the PLP interfacial modification of imogolite enables effective surface interactions between the imogolite fillers and the chitosan matrix, resulting in improved mechanical properties of the hybrid films.

Conclusions

In conclusion, imogolite surfaces were modified with the PLP *via* the interaction between the phosphate group of PLP and the Al-OH of the imogolite surface. The PLP-modified imogolite was characterized *via* UV-vis spectrometry, zeta-potential analysis, and TGA. Imogolite was used to prepare a hybrid film of chitosan. The formation of Schiff base linkages between PLP and chitosan was confirmed *via* UV-vis spectrometry and rheological measurements. The chitosan hybrid film exhibited superior mechanical properties, indicating that PLP acts as an interfacial modifier. Additionally, the hybrid material has great potential as an adsorbent because both chitosan and imogolite are promising materials for adsorbents.[9,14,20,24] Especially, the hybrid film may be particularly effective for metal adsorption. This is because PLP–Schiff base can form complexes with various metals,[30,34] and complexes of zinc and cadmium ions[41,42] have been reported to have strong fluorescence. Furthermore, adsorbents should be mechanically strong to withstand flowing wastewater. Thus, the present strategy can be applied for the development of a high-strength adsorbent.

Author contributions

Masaru Mukai: conceptualization, methodology, validation, investigation, writing – original draft; Akihiko Takada: investigation (rheological measurements); writing – original draft; Ayumi Hamada: investigation; Tomoko Kajiwara: investigation; Atsushi Takahara: resources, writing – review and editing, visualization, supervision, project administration and funding.

Conflicts of interest

There are no conflicts to declare.

Acknowledgements

The authors acknowledge the financial support of the JSPS Grant-in-Aid for Scientific Research (Grant No. 26248053 and 17H01221) and JSPS A3 Project.

Notes and references

1 O. Arnalds, in *Advances in Agronomy*, ed. D. L. Sparks, Academic Press, 2013, vol. 121, pp. 331–380.
2 P. D. G. Cradwick, V. C. Farmer, J. D. Russell, C. R. Masson, K. Wada and N. Yoshinaga, *Nat. Phys. Sci.*, 1972, **240**, 187–189.
3 K. Wada and N. Yoshinaga, *Am. Mineral.*, 1969, **54**, 50–71.
4 N. Yoshinaga and S. Aomine, *Soil Sci. Plant Nutr.*, 1962, **8**, 22–29.
5 J. Harsh, in *Encyclopedia of Soils in the Environment*, ed. D. Hillel, Elsevier, Oxford, 2005, pp. 64–71.
6 K. Wada and M. E. Harward, in *Advances in Agronomy*, ed. N. C. Brady, Academic Press, 1974, vol. 26, pp. 211–260.
7 V. C. Farmer, A. R. Fraser and J. M. Tait, *Chem. Commun.*, 1977, 462–463.
8 L. Lisuzzo, G. Cavallaro, G. Lazzara, S. Milioto, F. Parisi and Y. Stetsyshyn, *Appl. Sci.*, 2018, **8**, 1068.
9 Y. Arai, M. McBeath, J. R. Bargar, J. Joye and J. A. Davis, *Geochim. Cosmochim. Acta*, 2006, **70**, 2492–2509.

10 N. Inoue, H. Otsuka, S.-I. Wada and A. Takahara, *Chem. Lett.*, 2006, **35**, 194–195.
11 W. C. Ackerman, D. M. Smith, J. C. Huling, Y. W. Kim, J. K. Bailey and C. J. Brinker, *Langmuir*, 1993, **9**, 1051–1057.
12 E. Paineau, M.-E. M. Krapf, M.-S. Amara, N. V. Matskova, I. Dozov, S. Rouzière, A. Thill, P. Launois and P. Davidson, *Nat. Commun.*, 2016, **7**, 10271.
13 W. J. Lee, E. Paineau, D. B. Anthony, Y. Gao, H. S. Leese, S. Rouzière, P. Launois and M. S. P. Shaffer, *ACS Nano*, 2020, **14**, 5570–5580.
14 A. Takahara and Y. Higaki, in *Functional Polymer Composites with Nanoclays*, The Royal Society of Chemistry, 2017, pp. 131–156.
15 N. Jiravanichanun, K. Yamamoto, K. Kato, J. Kim, S. Horiuchi, W.-O. Yah, H. Otsuka and A. Takahara, *Biomacromolecules*, 2012, **13**, 276–281.
16 W. Ma, J. Kim, H. Otsuka and A. Takahara, *Chem. Lett.*, 2011, **40**, 159–161.
17 W. O. Yah, A. Irie, H. Otsuka, S. Sasaki, N. Yagi, M. Sato, T. Koganezawa and A. Takahara, *J. Phys.: Conf. Ser.*, 2011, **272**, 012021.
18 K. Yamamoto, H. Otsuka, A. Takahara and S.-I. Wada, *J. Adhes.*, 2002, **78**, 591–602.
19 M. Mukai, M. Takahara, A. Takada and A. Takahara, *RSC Adv.*, 2021, **11**, 4901–4905.
20 M. Rinaudo, *Prog. Polym. Sci.*, 2006, **31**, 603–632.
21 M. Hashizume, H. Kobayashi and M. Ohashi, *Colloids Surf., B*, 2011, **88**, 534–538.
22 P. Podsiadlo, L. Sui, Y. Elkasabi, P. Burgardt, J. Lee, A. Miryala, W. Kusumaatmaja, M. R. Carman, M. Shtein, J. Kieffer, J. Lahann and N. A. Kotov, *Langmuir*, 2007, **23**, 7901–7906.
23 K. M. A. Uddin, M. Ago and O. J. Rojas, *Carbohydr. Polym.*, 2017, **177**, 13–21.
24 R. Zhai, B. Zhang, Y. Wan, C. Li, J. Wang and J. Liu, *Chem. Eng. J.*, 2013, **214**, 304–309.
25 J. Karube, *Clays Clay Miner.*, 1998, **46**, 583–585.
26 Y. Lvov and E. Abdullayev, *Prog. Polym. Sci.*, 2013, **38**, 1690–1719.
27 Z. Jia, D. shen and W. Xu, *Carbohydr. Res.*, 2001, **333**, 1–6.
28 R. A. A. Muzzarelli, F. Tanfani, M. Emanuelli and S. Mariotti, *Carbohydr. Res.*, 1982, **107**, 199–214.
29 H. Tan, C. R. Chu, K. A. Payne and K. G. Marra, *Biomaterials*, 2009, **30**, 2499–2506.
30 M. Mukai, Y. Sasaki and J.-i. Kikuchi, *Sensors*, 2012, **12**, 5966–5977.
31 Y. Xin and J. Yuan, *Polym. Chem.*, 2012, **3**, 3045–3055.
32 M. Raven and P. Self, in *Clays in the Minerals Processing Value Chain*, ed. A. J. McFarlane, C. Klauber, D. J. Robinson and M. Gräfe, Cambridge University Press, Cambridge, 2017, pp. 142–204.
33 T. Maeda, H. Taguchi, H. Minami, K. Sato, T. Shiga, H. Kosaka and K. Yoshikawa, *Arch. Dermatol. Res.*, 2000, **292**, 562–567.
34 Y. Matsuo, *J. Am. Chem. Soc.*, 1957, **79**, 2011–2015.
35 E. I. Kozlov, M. S. L'Vova and V. V. Chugunov, *Pharm. Chem. J.*, 1979, **13**, 1164–1169.
36 F. Bartl, H. Urjasz and B. Brzezinski, *J. Mol. Struct.*, 1998, **441**, 77–81.
37 T. W. Geders, K. Gustafson and B. C. Finzel, *Acta Crystallogr., Sect. F: Struct. Biol. Cryst. Commun.*, 2012, **68**, 596–600.
38 M. Arrio-Dupont, *Biochem. Biophys. Res. Commun.*, 1971, **44**, 653–659.
39 S. A. Ahmed, P. McPhie and E. W. Miles, *J. Biol. Chem.*, 1996, **271**, 8612–8617.
40 D. Heinert and A. E. Martell, *J. Am. Chem. Soc.*, 1963, **85**, 183–188.
41 S. Bothra, L. T. Babu, P. Paira, S. K. Ashok Kumar, R. Kumar and S. K. Sahoo, *Anal. Bioanal. Chem.*, 2018, **410**, 201–210.
42 P. Riccio, S. Giovannelli, A. Bobba, E. Romito, A. Fasano, T. Bleve-Zacheo, R. Favilla, E. Quagliariello and P. Cavatorta, *Neurochem. Res.*, 1995, **20**, 1107–1113.